Forces between polymer brushes: Monte Carlo simulation of a continuous-space model

Raúl Toral,[1] Amitabha Chakrabarti,[2] and Ronald Dickman[3]
[1]*Institut d'Estudis Avançats and Departament de Física, Consejo Superior de Investigaciones Científicas and Universitat de les Illes Balears, 07071 Palma de Mallorca, Spain*
[2]*Department of Physics, Kansas State University, Manhattan, Kansas 66506*
[3]*Department of Physics and Astronomy, Herbert H. Lehman College, City University of New York, Bronx, New York 10468*
(Received 22 October 1993)

We present results of numerical simulations of a three-dimensional off-lattice model for polymer brushes end grafted to parallel planar surfaces, for several values of the surface coverage and the chain length. Besides computing the density profiles, we determine the force between the brushes, using an extension of a method originally devised for lattice systems. The results are compared with predictions of self-consistent field theory.

PACS number(s): 36.20.−r, 82.70.−y, 87.15.−v, 81.60.Jw

I. INTRODUCTION

In recent years considerable effort has been devoted to understanding how interactions between surfaces may be modified by terminally attaching polymer chains, via chemical bonding or adsorption [1]. This method has been used, for example, to stabilize colloidal suspensions by end grafting polymer chains onto the surface of the colloidal particles [2,3]. For surface coverages large enough to cause overlap of the chains, the end grafted chains adopt configurations rather different from the ones they have in solution, forming so-called *polymer brushes* [4]. The effective repulsion between two polymer brushes provides the force required to overcome van der Waals attractive forces between the particles and thus stabilization is achieved. The detailed structure of polymer brushes as well as the interactions between them have been the subject of recent experimental work [5–7], theoretical studies [8–11], and extensive computer simulations [12–19].

Among the theoretical approaches, the self-consistent-field (SCF) theory of Milner, Witten, and Cates [11] (MWC) has been quite successful in describing brushes. The parabolic density profile predicted by this theory has been confirmed in recent experiments and computer simulations. This theory also yields an expression for the force between two brushes, which has been confirmed qualitatively in molecular dynamics simulations and in Monte Carlo simulations of the fluctuating bond lattice model.

While most of the pertinent theories treat continuous-space models, Monte Carlo simulations of polymer brushes have mainly dealt with lattice models. Recently, however, Monte Carlo methods were applied to the structure and interactions of brushes in a freely jointed Lennard-Jones chain model [20,21] and to the configurational properties of a discretized Edwards's Hamiltonian [22]. The present work represents a further contribution to the study of more realistic, continuous-space models for polymer brushes [23–26]. We employ the freely jointed tangent hard-sphere model (or "pearl-necklace" model) for the chains [27]. The volumetric and configurational properties of this model are arguably the best understood of any off-lattice polymer model. This feature, together with computational simplicity, makes the pearl-necklace model a natural choice for the study of brushes. In this paper we present results of extensive computer simulations. We consider a pair of brushes in contact with one another, as well as a single brush compressed by a planar surface. In the former case, and in order to compute the pressure between brushes, the MWC theory assumes that there is no interpenetration between the chains. We observe, however, that some interpenetration does occur. We also compute the force needed for compressing the brush, using an extension of methods originally devised for lattice simulations [28,18]. We compare the results of the force measurements with the predictions of MWC.

The model and the simulation method are described in Sec. II. Section III presents the numerical results and their comparison with theoretical predictions. Section IV outlines the main conclusions.

II. MODEL AND SIMULATION METHOD

In order to compute the properties of interacting polymer brushes, we performed simulations of a three-dimensional off-lattice system, using the pearl-necklace model of flexible, linear polymer chains. In this model each monomer is represented by a hard sphere of diameter $a=1$. A chain consists of N monomers connected by rigid rods of length $1.1a$ between the sphere centers. Only excluded volume interactions are included, and so the model is athermal, i.e., all allowed configurations contribute equally in the partition function. The chains are enclosed within a box of dimensions $L_x \times L_y \times L_z$, with $L_x = L_y \equiv L = 40$ and $L_z = H$ varying from $H = 10$ to 120. The walls are impenetrable. The chains are grafted to one or both of the planes perpendicular to the z direction. Grafting is enforced by fixing the first monomer of each chain at a random position on either the $z=0$ or the $z=H$ plane, with the sphere center a distance of 0.5 from

the grafting plane. The surface coverage (number of grafted chains per unit area) is $\sigma = N_c/L^2$, N_c being the number of chains grafted to a wall. In the two-brush case only symmetric brushes—the same number of polymers on each plate—were studied. We considered several values of the surface coverage: $\sigma = 0.04$, 0.08, and 0.12 (corresponding, respectively, to 64, 128, and 192 chains per brush) and two chain lengths $N = 50$ and 100.

We sample the equilibrium probability distribution by generating a series of random monomer movements: end- or internal-bead jumps through a randomly chosen rotation angle. (The grafted monomers do not move.) A monomer displacement is accepted if the new position lies within the box and does not overlap any of the other monomers. We measure time in units of Monte Carlo steps per monomer (MCM). The initial configuration is equilibrated for at least 100 000 MCM for $N = 100$ and 50 000 MCM for $N = 50$. After this, the system is considered relaxed and the quantities of interest are averaged during a large number of configurations (typically more than 50 000 measurements). Successive measurements are taken at intervals of 10 MCM. Table I contains a summary of our runs.

When feasible, we started the simulation in an overlap-free, random configuration. But in systems with long chains, small separations between brushes, and/or high coverages, it was difficult to generate a nonoverlapping initial configuration. In such cases we found it useful to place the chains initially as self-avoiding random walks (no overlap between monomers on the same chain), but with the prohibition against interchain overlap relaxed. In the first stage of equilibration, only movements that produce no new overlaps are accepted. Eventually all overlaps are eliminated, providing a valid initial configuration, which is permitted to relax in the usual manner. We found this procedure more efficient than attempting to generate a random initial configuration satisfying all the excluded volume conditions from the beginning.

TABLE I. Summary of simulation parameters and measured pressures (the numbers in parentheses are the errors affecting the last two digits).

Run	N	σ	n	H	$\bar{P}$
1	50	0.04	2	100	0.0
2	50	0.04	2	40	0.002 90(58)
3	50	0.04	2	30	0.014 6(20)
4	50	0.04	2	20	0.058 7(34)
5	50	0.04	2	10	0.353(12)
6	50	0.08	2	100	0.0
7	50	0.08	2	40	0.419(14)
8	50	0.08	2	20	0.034 6(20)
9	50	0.12	1	100	0.0
10	50	0.04	1	20	0.005 90(70)
11	50	0.04	1	10	0.078 3(40)
12	50	0.08	1	20	0.041 8(14)
13	50	0.08	1	10	0.503(10)
14	50	0.12	1	20	0.149 0(25)
15	50	0.12	1	10	1.94(25)
16	100	0.04	1	100	0.0
17	100	0.08	1	100	0.0
18	100	0.12	1	120	0.0
19	100	0.04	1	20	0.059 0(75)
20	100	0.04	1	10	0.503(11)
21	100	0.08	1	20	0.444(16)

To compute the force in our simulations we employed an extension of a technique developed for lattice systems [28,18]. In this method one computes the change in free energy due to an infinitesimal compression ΔH. The pressure (in units of $k_B T$) is given by

$$\bar{P} \equiv \frac{P}{k_B T} = -\left[\frac{\partial F}{\partial V}\right]_T = L^{-2}\frac{\partial \ln Z}{\partial H}, \tag{1}$$

Z being the partition function of the system.

Consider a system with two brushes A and B grafted to the $z=0$ and H planes, respectively. (We refer to a chain grafted on the A plane as an A chain, comprised of A monomers, and similarly for the B plane.) Suppose there are N_A A monomers and N_B B monomers. (In our simulations $N_A = N_B = N_m$.) If Ω_H denotes the set of allowed configurations for a system with plate separation H, then the partition function $Z(H)$ is the volume $\mu[\Omega_H]$ of this set. Now let $\Omega^C_{H,\Delta H} \subset \Omega_H$ be the configurations which are still allowed when the distance between the walls is reduced to $H-\Delta H$ via a rigid translation of the brushes, i.e., all the monomers of the, say, A brush are rigidly translated towards the B brush. Similarly, let $\Omega^E_{H-\Delta H,\Delta H} \subset \Omega_{H-\Delta H}$ be the configurations in $\Omega_{H-\Delta H}$ which can be expanded to a distance H without overlap. Since these subsets are in one-to-one correspondence, $\mu[\Omega^C_{H,\Delta H}] = \mu[\Omega^E_{H-\Delta H,\Delta H}]$. The probability that such a compression can be done is

$$P^C_{H,\Delta H} = \frac{\mu[\Omega^C_{H,\Delta H}]}{Z(H)}, \tag{2}$$

and similarly for the expansion probability

$$P^E_{H,\Delta H} = \frac{\mu[\Omega^E_{H,\Delta H}]}{Z(H)}, \tag{3}$$

from one which deduces

$$\frac{Z(H-\Delta H)}{Z(H)} = \frac{P^C_{H,\Delta H}}{P^E_{H-\Delta H,H}}. \tag{4}$$

The expansion and compression probabilities are readily evaluated from two-body correlation functions. Define $g_{ij}(r,\theta)$ such that $g_{ij}(r,\theta)dr d\theta$ is the probability of finding the ith A monomer and the jth B monomer at a distance interval $(r, r+dr)$ and angle interval $(\theta, \theta+d\theta)$, with θ reckoned with respect to the $-z$ direction. Particles i and j overlap upon compression if $r^2+(\Delta H)^2-2r\Delta H\cos\theta < a^2$ (see Fig. 1). In the limit $\Delta H \to 0$, the overlap condition becomes $r < a+\Delta H\cos\theta$.

The probability $P^{\bar{C}}(i,j)$ that the ith A monomer and the jth j do not allow compression, i.e., that $r_{ij} \le a+\Delta H\cos\theta$, is

$$P^{\bar{C}}(i,j) = \int_0^{\pi/2}\int_a^{a+\Delta H\cos\theta} g_{ij}(r,\theta)dr\, d\theta \tag{5}$$

$$\approx \Delta H \int_0^{\pi/2} g_{ij}(a,\theta)\cos\theta\, d\theta \tag{6}$$

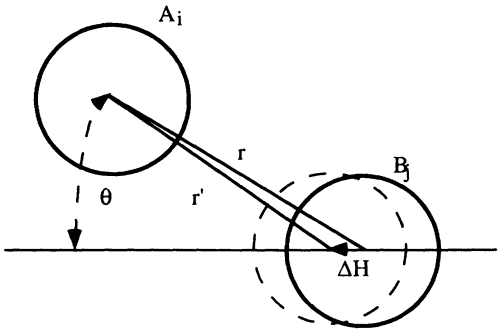

FIG. 1. Schematic of a particle displacement in a virtual compression.

to leading order as $\Delta H \to 0$. In this limit, the probability that the separation between the walls can be reduced by ΔH is the product over all A-B pairs of the probability that a particular pair allows compression:

$$P^C_{H,\Delta H} = \prod_{i=1}^{N_A} \prod_{j=1}^{N_B} [1 - P^{\bar{C}}(i,j)] \ . \tag{7}$$

Using Eq. (6) one can expand the logarithm of the right-hand side to order ΔH and write

$$\ln(P^C_{H,\Delta H}) = -\Delta H \int_0^{\pi/2} \sum_{i=1}^{N_A} \sum_{j=1}^{N_B} g_{ij}(a,\theta) \cos\theta \, d\theta \ . \tag{8}$$

Finally, defining

$$G_{AB}(r,\theta) = \sum_{i=1}^{N_A} \sum_{j=1}^{N_B} g_{ij}(r,\theta) \ , \tag{9}$$

one obtains

$$\ln(P^C_{H,\Delta H}) = -\Delta H \int_0^{\pi/2} G_{AB}(a,\theta) \cos\theta \, d\theta \ . \tag{10}$$

$G_{AB}(r,\theta) dr \, d\theta$ represents the average number of A-B pairs with separation in the interval $(r, r+dr)$ and angle in the interval $(\theta, \theta+d\theta)$.

In the same way, one obtains the probability of expansion

$$\ln(P^E_{H-\Delta H,\Delta H}) = -\Delta H \int_{\pi}^{\pi/2} G_{AB}(a,\theta) \cos\theta \, d\theta \ . \tag{11}$$

By using the relation

$$\frac{\partial \ln Z(H)}{\partial H} = \lim_{\Delta H \to 0} \frac{-1}{\Delta H} \ln \left[\frac{Z(H-\Delta H)}{Z(H)} \right] , \tag{12}$$

one gets the following final expression for the reduced pressure:

$$\bar{P} = \bar{P}(r=a) \ , \tag{13}$$

where we have defined the function

$$\bar{P}(r) = L^{-2} \int_0^{\pi} G_{AB}(r,\theta) \cos\theta \, d\theta \ . \tag{14}$$

In the simulation, the above integral is approximated by the sum

$$\bar{P}(r) = \frac{L^{-2}}{\Delta r N_{\text{meas}}} \sum_{i=1}^{N_A} \left\{ \sum_{j \ B \text{ particles such that } r \le r_{ij} \le r+\Delta r} \cos\theta_{ij} \right\} , \tag{15}$$

where θ_{ij} is the angle between $\mathbf{r}_j - \mathbf{r}_i$ and the $-z$ direction, and N_{meas} is the number of measurements. The bin size Δr is typically 0.01. Once the function $\bar{P}(r)$ has been computed, a simple straight line fit for small values of r allows a smooth extrapolation towards $r=a$.

The derivation for the single brush case follows essentially the same lines, the main difference being that the probability of extension is always 1. The resulting expression is

$$\bar{P} = L^{-2} G(r = a/2) \ , \tag{16}$$

where

$$G(r) = \sum_{i=1}^{N} g_i(r) \tag{17}$$

and $g_i(r)dr$ is the probability that the distance between monomer i and the wall lies in the interval $(r, r+dr)$.

III. RESULTS

A. Density profile

We first analyze the segment density profile of a "free" brush (i.e., a brush unperturbed by contact with another brush or wall), which provides us with the excluded volume parameter ω needed for comparison with MWC theory. This theory predicts a parabolic density profile

$$\phi(z) = \left[\frac{9\pi^2\sigma^2}{32\omega} \right]^{1/3} - \frac{\pi^2}{8N^2\omega} z^2 \tag{18}$$

for $z \le h^*$ and $\phi(x) = 0$ for $z > h^*$, where the height is

$$h^* = N \left[\frac{12\sigma\omega}{\pi^2} \right]^{1/3} . \tag{19}$$

The density profile may be cast in the simple scaling form

$$\frac{\phi(z)}{\sigma^{2/3}} = F^{\phi}_{\omega} \left[\frac{z}{N\sigma^{1/3}} \right] , \tag{20}$$

where the scaling function $F^{\phi}_{\omega}(x)$ depends only on the parameter ω, not on surface coverage or chain length.

In Fig. 2 we have plotted the density profiles of uncompressed brushes ($\sigma = 0.04, 0.08, 0.12$ and $N = 50, 100$) using the scaled variables of Eq. (20). This figure shows that the scaling description holds well for the surface coverages and chain lengths considered here. (This shows that the system is sufficiently large that global

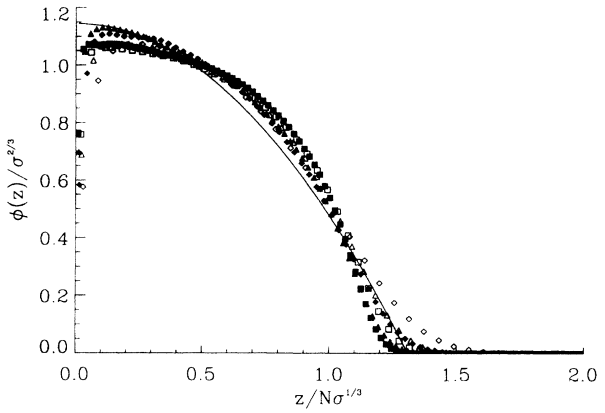

FIG. 2. Density profiles of free brushes, plotted in the rescaled variables of Eq. (20). The symbols are as follows (see Table I for run numbers): empty diamonds, run 1; empty triangles, run 6; empty squares, run 9; filled diamonds, run 16; filled triangles, run 17; and filled squares, run 18. The solid line is the prediction of MWC theory using $\omega=1.85$.

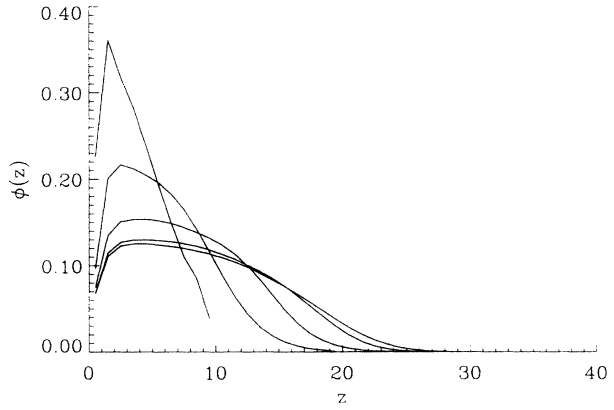

FIG. 3. Density profiles of an A brush (grafted to the $z=0$ plane), in contact with a similar B brush (grafted to the $z=H$ plane), for surface coverage $\sigma=0.04$ and chain length $N=50$. The separation is, from top to bottom, $H=10,20,30,40,100$. ($H=100$ represents a free brush.)

properties are not significantly perturbed by the walls perpendicular to the brush.) Also, beyond the density maximum, the parabolic profile offers a reasonable fit to the data, although the best value for ω, obtained from a least-squares fit, slightly varies from run to run. From the best-fit values and their dispersion we obtain

$$\omega=1.85\pm0.15\ . \tag{21}$$

In Fig. 2 the solid line represents the function $F_{\omega}^{\phi}(x)$ taking the above value of ω. We note that the agreement between the theoretical prediction and the numerical results is reasonably good for $\sigma=0.04$ and 0.08. On the other hand, the profile for $\sigma=0.12$ exhibits a plateau near the grafting surface and deviates considerably from the parabolic profile. The fact that, for increasing coverages, there should be a deviation from the parabolic profile is predicted by the work of Zhulina, Borisov, and Priamitsyn [29] in which higher terms in the virial expansion for the equation of state are considered. However, we have not tried a quantitative comparison with the results of this theory since, for the purpose of this paper, comparison with the simpler theory of MWC suffices to determine accurately the excluded volume interaction parameter ω. A more detailed comparison with the results of Zhulina, Borisov, and Priamitsyn would imply measuring the chemical potential, which should remain parabolic even for large coverages. Measuring the chemical potential would be quite involved though, since one would have to determine the insertion probability for a monomer of a partially grown chain.

We consider now the case of two brushes (under the same conditions of surface coverage and chain length) a distance H apart. When the distance between the plates H is larger than the single brush maximum length h^*, the brush profile is unaffected by the presence of the other brush; for $H<h^*$, the brushes are compressed. According to the MWC theory, the scale over which penetration does occur is small in the strong-stretching limit and the parabolic profile is maintained, except that now the parameter h^* is reduced from the original free brush value. In the simulation, however, we observe that some interpenetration does occur and the quality of the parabolic fit to the density profile worsens with decreasing d. In Fig. 3 we plot the density profile of one of the brushes (the other is symmetric with respect to the $z=H/2$ axis) for coverage $\sigma=0.04$ and chain length $N=50$, clearly showing the compression produced on the brush as the separation is reduced from $H=100$ (independent brushes) to 10 (strong compression). For this case the equilibrium height is, according to Eq. (19), $h^*=22.4$. To show the interpenetration effect, we have plotted in Fig. 4 the density profile for each brush and the total density profile in the case $\sigma=0.04$, $N=50$, and separation between plates $H=20$. In this case the total monomer concentration is almost a constant in between the planes.

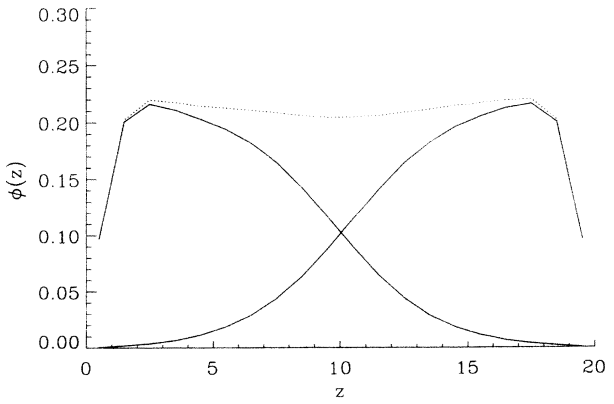

FIG. 4. Density profiles for each brush (continuous lines) in the case of surface coverage $\sigma=0.04$, chain length $N=50$, and separation between plates $H=20$ to show the interpenetration effect present at this close distance between plates. The dotted line is the total monomer concentration.

B. Force between plates

To begin, we summarize the predictions of the MWC theory for the force between brushes. Although the original derivation is for the two-brush problem ($n=2$), it can be readily extended to treat a brush in contact with a wall ($n=1$). According to this theory, the free energy per chain $\mathcal{F}$, in arbitrary units, is given by

$$\mathcal{F}=N\left[\frac{\pi^2}{12}\right]^{1/3}(\sigma\omega)^{2/3}\left[\frac{u^2}{2}-\frac{1}{2u^2}-\frac{u^5}{10}\right], \tag{22}$$

where $u=H/(nh^*)$ and h^* is the unperturbed brush height given by Eq. (19). The total free energy is $F=nN_c\mathcal{F}$. From this expression for the free energy, the pressure can be obtained from the thermodynamic relation

$$P=-\left[\frac{\partial F}{\partial V}\right]_T. \tag{23}$$

For the geometry we are considering, the volume is $V=L^2H$, from which one obtains

$$P=\tfrac{1}{2}(\sigma^4\omega)^{1/3}\left[\frac{\pi^2}{12}\right]^{2/3}\left[u^2-\frac{1}{u}\right]^2. \tag{24}$$

In order to stress the scaling properties of this theoretical prediction we introduce the reduced variables

$$P^*=\frac{P}{\sigma^{4/3}} \tag{25}$$

and

$$x=\frac{H}{n\sigma^{1/3}N}, \tag{26}$$

in terms of which we may write

$$P^*=F_\omega(x), \tag{27}$$

where $F_\omega(x)$ is a universal function which depends only on the parameter ω, not on chain length, number of brushes, etc. It is given by

$$F_\omega(x)=\frac{\pi^2}{24}a_2\left[\left[\frac{x}{a_2}\right]^2-\frac{a_2}{x}\right]^2, \tag{28}$$

where

$$a_2=\left[\frac{12\omega}{\pi^2}\right]^{1/3}. \tag{29}$$

Our results for the pressure are listed in Table I. As expected, the pressure decreases monotonically with increasing H and is zero when the distance H between the plates is greater than twice the single brush height. In order to compare our results with the MWC prediction, we have plotted in Fig. 5 the data for the pressure in the rescaled variables of Eq. (28). The scaling relation is seen to hold reasonably well for both the single brush and two-brush cases, although it seems to worsen with decreasing H. Note that in Eq. (28) the pressure is given in arbitrary units, whereas our simulation measures pressure in units of k_BT, so that a comparison between the MWC prediction simulation involves an arbitrary prefactor. The solid line in Fig. 5 represents Eq. (28) (with $\omega=1.85$ obtained from the density profile fits), multiplied by a scaling factor 3.1, adjusted via a least-squares fit.

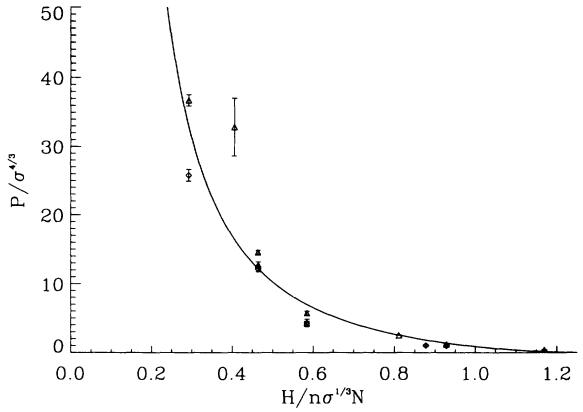

FIG. 5. Scaling plot of the pressure. The triangles correspond to $n=1$) (one brush), the diamonds to $n=2$. The solid line represents Eq. (28) with a prefactor chosen to best fit the data.

IV. CONCLUSIONS

We have performed Monte Carlo simulations of a three-dimensional off-lattice pearl-necklace model for polymer brushes, focusing on the density profile and the interaction between brushes and between a brush and a wall. We considered surface coverages ranging from $\sigma=0.04$ to 0.12 and chain lengths of $N=50$ and 100. Our results support the SCF theory predictions of MWC in that we obtain a parabolic density profile over most of the brush. However, the density profile shows a depletion zone near the origin, not predicted by MWC theory. Direct comparison with the MWC expression allows us to compute the excluded volume interaction parameter $\omega=1.85\pm0.15$. We have also studied the compression produced when two brushes are brought into contact. In this case, in contrast to the assumptions used in the theory to compute the force between the brushes, some brush interpenetration does occur.

We derived an expression relating the force between two brushes (or between a brush and a nongrafted plane) to the value of an orientational correlation function at contact. Our results for the pressure support the scaling prediction of MWC. Moreover, an analytical expression for the scaling function containing only one adjustable

parameter fits the data for a wide range of surface coverages and chain lengths.

ACKNOWLEDGMENTS

Financial support from the Dirección General de Investigación Científica y Técnica (Spain), Grant No. PB-92-0046, is acknowledged. This material is based upon work supported by the National Science Foundation under Grant No. OSR-9255223 (NSF-EPSCoR) at Kansas State University (KSU). This work also received matching support from the state of Kansas. R.T. acknowledges the warm hospitality at the Department of Physics, KSU, where part of this work was carried out.

[1] A recent review is given in S. T. Milner, Science **251**, 905 (1991).
[2] See, for example, D. H. Napper, *Polymeric Stabilization of Colloidal Dispersions* (Academic, London, 1983).
[3] W. B. Russel, D. A. Saville, and W. R. Schowalter, *Colloidal Dispersions* (Cambridge University Press, Cambridge, 1989).
[4] A. Halperin, M. Tirrell, and T. P. Lodge, Adv. Polymer Sci. **100**, 31 (1992).
[5] H. J. Taunton, C. Toprakcioglu, L. J. Fetters, and J. Klein, Nature **332**, 712 (1988).
[6] P. Auroy, L. Auvray, and L. Leger, Phys. Rev. Lett. **66**, 719 (1991).
[7] P. Auroy, Y. Mir, and L. Leger, Phys. Rev. Lett. **69**, 93 (1992).
[8] S. Alexander, J. Phys. (Paris) **38**, 983 (1977).
[9] P. G. de Gennes, Adv. Colloid Interface Sci. **27**, 189 (1987); Macromolecules **13**, 1069 (1980).
[10] A. N. Semenov, Zh. Eksp. Teor. Fiz. **88**, 1242 (1985) [Sov. Phys. JETP **61**, 733 (1985)].
[11] S. T. Milner, T. A. Witten, and M. E. Cates, Macromolecules **21**, 1610 (1988); **22**, 853 (1989).
[12] T. Cosgrove, T. Heath, B. van Lent, F. Leermakers, and J. Scheutjens, Macromolecules **20**, 1692 (1987).
[13] M. Muthukumar and J. S. Ho, Macromolecules **22**, 965 (1989).
[14] A. Chakrabarti and R. Toral, Macromolecules **23**, 2016 (1990); R. Toral and A. Chakrabarti, Phys. Rev. E **47**, 4240 (1993).
[15] A. Chakrabarti, P. Nelson, and R. Toral, Phys. Rev. A **46**, 4930 (1992); J. Chem. Phys. **100**, 748 (1994); J. F. Marko and A. Chakrabarti, Phys. Rev. E **48**, 2739 (1993).
[16] P.-Y. Lai and K. Binder, J. Chem. Phys. **95**, 9288 (1991).
[17] P.-Y. Lai and K. Binder, J. Chem. Phys. **97**, 586 (1992).
[18] R. Dickman and D. Hong, J. Chem. Phys. **95**, 4650 (1991).
[19] M. Murat and G. Grest, Macromolecules **22**, 4054 (1989).
[20] L. J. Gallego, C. Rey, and M. J. Grimson, Mol. Phys. **74**, 383 (1991).
[21] M. J. Grimson, Chem. Phys. Lett. **180**, 129 (1991).
[22] M. Laradji, H. Guo, and M. J. Zuckermann, Phys. Rev. E **49**, 3199 (1994).
[23] I. Carmesin and K. Kremer, Macromolecules **21**, 2819 (1988).
[24] H.-P. Deutsch and R. Dickman, J. Chem. Phys. **93**, 8983 (1990).
[25] H.-P. Deutsch and K. Binder, J. Chem. Phys. **94**, 2294 (1991).
[26] R. Dickman and P. E. Anderson, J. Chem. Phys. **99**, 3112 (1993).
[27] A. Baumgärtner, in *Applications of the Monte Carlo Method*, edited by K. Binder (Springer-Verlag, Berlin, 1987), p. 145.
[28] R. Dickman, J. Chem. Phys. **86**, 2246 (1987).
[29] E. Zhulina, O. Borisov, and V. Priamitsyn, J. Colloid Interface Sci. **137**, 495 (1990).